Fluorescence Depolarization and Temperature Dependence of the Torsion Elastic Constant of Linear ϕ29 Deoxyribonucleic Acid†

John C. Thomas* and J. Michael Schurr

ABSTRACT: The torsion elastic constant α of linear ϕ29 DNA has been determined as a function of temperature from 10 to 78 °C by studying the decay of the fluorescence polarization anisotropy (FPA) of intercalated ethidium dye. The time-dependent FPA was measured by using a picosecond dye laser for excitation and time-correlated single photon counting detection. Over the region 10–74 °C, α was effectively constant within experimental error, varying from $(3.5 \pm 0.4) \times 10^{-12}$ dyn cm at 10 °C to $(3.7 \pm 0.3) \times 10^{-12}$ dyn cm at 74 °C. At 78 °C, which is just above the melting temperature $T_m = 76$ °C, α decreased to $(3.3 \pm 0.3) \times 10^{-12}$ dyn cm, and at 90 °C, where the DNA is completely denatured, both the fluorescence lifetime and the decay time of the FPA are characteristic of unbound ethidium bromide. The weak temperature dependence of α implies that DNA torsional deformations do not occur primarily at sites of high enthalpy perturbed structures such as open base pairs.

In the first time-resolved studies of the fluorescence polarization anisotropy (FPA) of ethidium/DNA complexes, Wahl et al. (1970) observed a rapid relaxation on a time scale ≤28 ns, which they ascribed to torsional motions of the DNA. A theory of the torsion dynamics and FPA of elastically deformable filaments was developed subsequently by Allison & Schurr (1979) for a connected-rod model with arbitrary rod and contour lengths. Independently, Barkley & Zimm (1979) developed a theory for the limiting case of short rods and long contour lengths. In the same paper, Barkley and Zimm also presented an approximate theory for small mean-squared angular displacements of the helix axis due to bending. The correct expression for the FPA in terms of mean-squared angular displacements due to both torsions and tumbling of the helix axis was subsequently obtained for the case of rigid axes (Allison et al., 1982; Schurr, 1982) and nonrigid axes (Schurr, 1983a). The corresponding FPA formula presented by Barkley and Zimm is incorrect, except when the tumbling (bending) contribution vanishes.

Using a picosecond laser system, we showed previously (Thomas et al., 1980a) that the FPA of ϕ29 DNA followed closely the highly nonexponential decay predicted for the torsion dynamics of long filaments with sufficiently short rod lengths and specifically ruled out rod lengths from 20 to 1000 base pairs. In the same paper, we reported the first quantitative determination of the (effective) torsion elastic constant (α) of DNA. Subsequent work with time-resolved FPA (Millar et al., 1982; Wilcoxon et al., 1982; Genest et al., 1982) and also transient photodichroism (Hogan et al., 1982; Wang et al., 1982) demonstrates the great potential of pulsed optical techniques for probing DNA torsion dynamics and rigidity under a wide variety of conditions.

Here we determine the temperature dependence of α in order to assess the possible contribution of high enthalpy perturbed structures to spontaneous torsional deformations. This work is also part of a broader effort to establish a firm connection between FPA measurements and other physical techniques used to monitor the short-wavelength dynamics and rigidities of DNA, such as dynamic light scattering (DLS) at ultraviolet wavelengths (Thomas & Schurr, 1979; Thomas et al., 1980b; Lin et al., 1981; Wilcoxon et al., 1982; Wilcoxon & Schurr, 1983; Schurr, 1983b) and electron paramagnetic resonance (EPR) spectroscopy with spin-labeled intercalators (Robinson et al., 1980). Both DLS (Wilcoxon & Schurr, 1983) and EPR (Robinson et al., 1980) studies of DNA as a function of temperature (T) have been reported previously and are discussed below. A theory describing the effect of occasional high-enthalpy disruptions of the local secondary structure on the temperature dependence of the apparent twisting rigidity is given elsewhere (Wilcoxon & Schurr, 1983). The implications of present and earlier results for the model recently proposed by Manning (1983) are discussed below.

Materials and Methods

DNA Samples. A concentrated stock solution (2 mg/mL) of linear ϕ29 DNA (M_r 11.5×10^6) was prepared in the manner described previously (Thomas et al., 1980b; Lin et al., 1981). The homogeneity of this preparation was checked by gel electrophoresis in 0.3% agarose. Under both neutral and denaturing conditions, the DNA ran as a sharp single band, indicating a narrow molecular weight distribution and an insignificant number of single-strand breaks. A fluorescamine test on this sample indicated a reasonably low level of protein contamination. This was supported by a dynamic light scattering measurement on the sample that gave a "normal" value (10.5×10^{-12} m^2 s^{-1}) for the apparent diffusion coefficient D_{plat} at large scattering vector. The ratio of the absorbance of the sample at 260 nm to that at 280 nm was $A_{260}/A_{280} = 1.87$, which is further indication of a low level of protein contamination. Previously (Wilcoxon & Schurr, 1983), we found that DNA does not degrade during extended periods at elevated temperatures, if it is dissolved in 0.1 M NaCl + 0.02 M ethylenediaminetetraacetic acid (EDTA) + 0.01 M tris(hydroxymethyl)aminomethane (Tris) buffered to pH 8.5. For the present work, the DNA was simply diluted to a concentration of 0.05 mg/mL in this buffer, and ethidium bromide was added to a final concentration of 0.1 μg/mL. This gives a DNA phosphate/dye ratio of approximately 600, which is the same dye coverage as previously used (Thomas et al., 1980a).

Fluorescence Anisotropy Measurements. (A) Instrumentation. These measurements were performed with a picosecond pulsed dye laser for excitation and time-correlated single-photon counting for detection of the ethidium fluorescence emission. The excitation wavelength was 575 nm, and the

† From the Department of Chemistry, University of Washington, Seattle, Washington 98195. *Received June 13, 1983.* This work was supported in part by Grant GM29338-01 from the National Institutes of Health.

0006-2960/83/0422-6194$01.50/0

fluorescence emission beyond 630 nm was collected. A detailed description of this system has already been given (Thomas et al., 1980a). The only changes implemented since then are that the system is now on-line to a VAX 11/780 computer for data processing and we now collect 1024 pulse height analyzer channels instead of 512 channels.

The quartz sample cuvette was enclosed in a jacketted housing, and the temperature of the sample was controlled by pumping water at a set temperature through the housing. The water was supplied and its temperature controlled by a VWR Model 90T water bath.

(*B*) *Data Analysis.* Our data analysis technique has been described (Thomas et al., 1980a), and we give only a brief outline of the procedure here. The measured decay curves for the sum or total fluorescence $s(t)$ and the difference between the two fluorescence polarization components $d(t)$ are convolutions of the measured instrument response function $e(t)$ and the true decay curves $S(t)$ and $D(t)$, respectively. Nonlinear least-squares fitting by a convolute-and-compare approach is used to determine the best fit curves for $S(t)$ and $r(t) = S(t)/D(t)$. Here, $r(t)$ is the time-dependent fluorescence polarization anisotropy, which describes the torsional motion of the duplex DNA. $S(t)$ was simply fitted to an exponential decay (or a sum of exponentials), and $r(t)$ was fitted to the Intermediate Zone functional form given by Allison & Schurr (Allison & Schurr, 1979)

$$r(n) = r_0[a_1 + a_2 \exp(-C_2 n^{1/2}) + a_3 \exp(-4C_2 n^{1/2})] \quad (1)$$

Here, n is the channel number of the pulse height analyzer, which is proportional to time, $t = n\Delta t$, where Δt is the precisely known channel delay time. a_1, a_2, and a_3 are known geometric constants (Thomas et al., 1980a) that depend solely on the binding angle between the transition dipole moment of the ethidium cation and the local helix axis. We assume that this angle remains fixed at 70.5°. The initial anisotropy r_0 (ideally 0.4) and the parameter

$$C_2 = \frac{k_B T \Delta t^{1/2}}{(\pi \alpha \gamma)^{1/2}} \quad (2)$$

are extracted in the fitting process. Here, k_B is the Boltzmann constant, T is the absolute temperature, α is the torsion spring constant between rods of length one base pair, and γ is the friction factor for azimuthal rotation about the symmetry axis of a one base pair rod. The value for α is calculated from the best fit value of C_2 with the relationship given in eq 2. The rotational friction factor for a one base pair rod is determined from $\gamma = 4\pi\eta a^2 h$, where $h = 0.34$ nm is the length and $a = 1.2$ nm is the radius of a base pair.

This analysis ignores any contribution of helix-axis reorientation to the anisotropy decay in the 120 ns following the laser excitation pulse. Recent Brownian simulations by Allison & McCammon (1983), as well as analytical and empirical considerations to be presented elsewhere, indicate that the Barkley–Zimm theory substantially overestimates the mean-squared angular displacement $\langle \Delta_x(t)^2 \rangle$ of the helix axis in this time range. For that reason, we presently neglect this comparatively small contribution. When a satisfactory analysis of the bending contribution ultimately becomes available, our measured torsion constants can be corrected merely by applying a scale factor in the range 1.0–1.62. The latter extreme results from using the Barkley–Zimm formula for $\langle \Delta_x(t)^2 \rangle$ (J. Shibata, unpublished results).

Results and Discussion

Fluorescence Decay. Over the temperature range 10–74 °C, the total fluorescence could be fitted to two exponentials.

Table I: Temperature Dependence of Best Fit Fluorescence Lifetimes and Anisotropy Decay Parameters

T (°C)	τ_A (ns)	τ_B (ns)	r_0	C_2
10	22.38 ± 0.04		0.345 ± 0.003	0.012 ± 0.003
20	22.15 ± 0.03		0.342 ± 0.002	0.014 ± 0.001
40	21.16 ± 0.02		0.350 ± 0.007	0.019 ± 0.001
50	20.64 ± 0.05		0.345 ± 0.007	0.021 ± 0.001
60	19.97 ± 0.03		0.345 ± 0.008	0.023 ± 0.001
70	19.42 ± 0.04		0.310 ± 0.007	0.023 ± 0.001
74	19.06 ± 0.05		0.303 ± 0.005	0.026 ± 0.001
78	18.69 ± 0.05	1.43 ± 0.04	0.287 ± 0.005	0.029 ± 0.001
90		1.33 ± 0.01	0.166 ± 0.005	0.148 ± 0.007

The dominant component had a lifetime in the range 19–22 ns and was due to emission from intercalated ethidium. The other component, which varied greatly in amplitude, had a lifetime in the range 100–200 ps and could be eliminated completely by shifting the raw pulse height analyzer data by one or two channels. We ascribe this short lifetime, which is far too short to be attributed to emission from unbound ethidium (see Temperature Dependence of the DNA Torsion Constant), to small intermittent timing drifts in our detection system. At 78 °C, a further decay component with a lifetime of 1.4 ns appeared in the fluorescence data. This component, which had an amplitude approximately one-third as large as the predominant long time component, we attribute to fluorescence emission from free ethidium cation. Finally, at 90 °C the fluorescence decay is totally dominated by emission from the unbound ethidium. In Table I we summarize the results of curve fitting to the fluorescence data for each temperature studied. τ_A and τ_B are the fluorescence lifetimes, and we have ignored the 100–200-ps artifactual lifetime. Also shown in the table are the best fit anisotropy decay parameters r_0 and C_2 for each temperature.

DNA Uniformity. As a matter of course when doing these measurements, we check that the Intermediate Zone model (IZM) accurately describes the depolarization dynamics of the DNA sample. This is done by doing the FPA experiment on different time scales and examining the variation of the best fit model parameters (r_0, C_2) with experimental time span. In Figure 1 we have plotted α (calculated from C_2) and r_0 as a function of channel delay time for Δt = 10.3, 20.0, 40.4, and 80.0 ps per channel, which correspond to time spans of 10, 20, 40, and 80 ns, respectively. These measurements were made at 20 °C, and each point is the mean value from a set of five measurements. The error bars represent the standard error of the mean for each data set. The data show very little variation with time span, indicating that the IZM anisotropy formula describes precisely the depolarization dynamics of this DNA. This in turn implies that ϕ29 DNA behaves as a torsionally smooth elastic filament with no widely separated torsion joints (Thomas et al., 1980a).

The mean value obtained by averaging the data from all experiments on different time spans is $\bar{\alpha} = (3.51 \pm 0.2) \times 10^{-12}$ dyn cm. This is slightly smaller than the value reported previously (Thomas et al., 1980a) due to the higher NaCl concentration used in the present work.

Temperature Dependence of the DNA Torsion Constant. Figure 2 shows the variation of α, calculated from the data in Table I, with temperature over the range 10–90 °C. These values are obtained from FPA measurements by using just a single-channel delay, Δt = 80.0 ps/channel. To complete these measurements in a reasonable period of time, we chose to measure the FPA data at Δt = 80.0 ps/channel, because this time scale consistently gives the best signal-to-noise ratio and

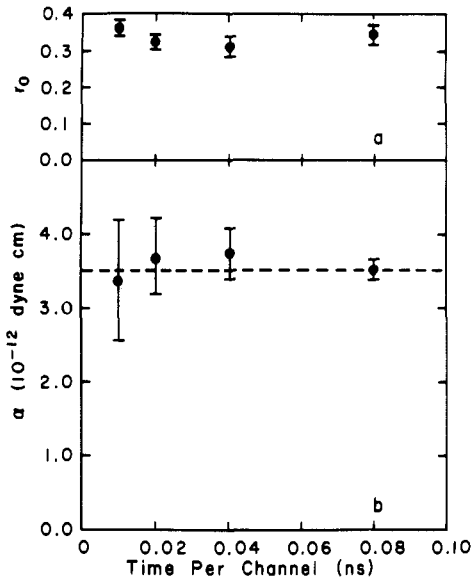

FIGURE 1: Variation of DNA torsion elastic constant α and initial anisotropy r_0 with experimental time resolution. The broken line in (b) indicates the mean value $\bar{\alpha} = (3.51 \pm 0.2) \times 10^{-12}$ dyn cm. ϕ29 DNA was 0.05 mg/mL in 0.1 M NaCl + 0.02 M EDTA + 0.01 M Tris, pH 8.5.

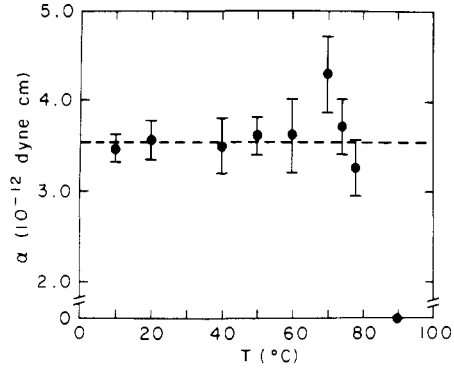

FIGURE 2: Variation of DNA torsion elastic constant α with temperature. ϕ29 DNA was 0.05 mg/mL in 0.1 M NaCl + 0.02 M EDTA + 0.01 M Tris, pH 8.5. For comparison, the mean value $\bar{\alpha}$ obtained from Figure 1 is shown by the broken line.

this time range covers very well the time course of the fluorescence decay. A nonuniform torsional rigidity was previously induced in ϕ29 DNA by binding spermidine at pH 10.2, thereby producing elastic weaknesses in the range $\sim 1/300$ base pairs. This nonuniformity was manifested primarily at the longer time scales, 80 and 120 ns, where α was substantially reduced (Wilcoxon et al., 1982). Thus FPA measurements with $\Delta t = 80.0$ ps/channel should provide a most sensitive monitor of the temperature dependence of the torsional rigidity. As above, each point is the mean value obtained from five different measurements, and the error bars indicate the standard error of the mean.

We see immediately from Figure 2 that over the temperature range 10–74 °C, which is close to the melting temperature $T_m = 76$ °C, the measured value of α changes very little and, indeed, is within experimental error of the value $\bar{\alpha} = 3.51 \times 10^{-12}$ dyn cm obtained from Figure 1. There is apparently no uniform increase or decrease in α with temperature over this range. Even at 78 °C, which is above the T_m for this DNA, the value for α is within experimental error of the value obtained at room temperature. That α must be nearly independent of T was inferred previously from DLS at studies on the basis of an *empirical* connection between the plateau diffusion coefficient (D_{plat}) at large scattering vector and α (Wilcoxon & Schurr, 1983). Likewise, EPR data over a more limited temperature range (Robinson et al., 1980) can be interpreted to imply a constant α. The present data provide a rigorous and quantitative basis for those conclusions.

At 90 °C, the fluorescence intensity (count rate) decreased to a value of $\sim 1/13$ the intensity at 78 °C, and the predominant fluorescence lifetime shortened dramatically to 1.33 ± 0.01 ns, which is close to the value of 1.32 ± 0.01 ns that we measure for ethidium bromide in water at 90 °C. The decreased fluorescence quantum yield and lifetime indicate that the DNA is fully denatured and we are essentially seeing free ethidium bromide in solution. The value for α at 90 °C shown on the figure is obtained by fitting the anisotropy data to the IZM formula in the usual way. Even though this model is not appropriate for the free diffusion of unbound ethidium, it does provide us with some kind of a value for α (if the ethidium were still rigidly attached to the DNA) for comparison with our lower temperature data. This value is $\alpha = 0.015 \times 10^{-12}$ dyn cm (i.e., 200 times smaller than the value that prevails at temperatures below T_m).

From Table I we can see that at 70 °C the initial anisotropy begins to decrease from the value $r_0 = 0.345$ that prevails at lower temperatures. This decrease may be attributed to an increasing fraction of very fast (subnanosecond) depolarization associated with an increasing concentration of unbound ethidium at higher temperatures.

Implications of a Temperature-Invariant Torsion Elastic Constant. If the *overall* torsional rigidity is significantly diminished by occasional perturbed structures of high enthalpy, such as single open base pairs, then the measured value of α must be strongly temperature dependent. This can be seen formally as follows. An overall α can always be defined in terms of the mean twisting persistence length w according to

$$\alpha = [k_B T/(2h)]w = \frac{k_B T}{f\langle\phi^2\rangle_d + (1-f)\langle\phi^2\rangle_o} \qquad (3)$$

which is valid for $\langle\phi^2\rangle_d \ll 1$ and $\langle\phi^2\rangle_o \ll 1$ (Wilcoxon & Schurr, 1983). In eq 3, f is the fraction of perturbed or disrupted base pairs, ϕ is the azimuthal angular displacement in radians between a particular base pair and its successor, and $\langle\phi^2\rangle_d$ and $\langle\phi^2\rangle_o$ are averages corresponding to disrupted and unperturbed base pairs, respectively. A significant reduction in α is effected only when (1) $\langle\phi^2\rangle_d$ is appreciably greater than $\langle\phi^2\rangle_o$ and (2) f is sufficiently large that $f\langle\phi^2\rangle_d$ is not negligible compared with $(1-f)\langle\phi^2\rangle_o$. Under these conditions the temperature dependence of α will reflect to a considerable extent the temperature dependence of $f\langle\phi^2\rangle_d$. In general, $f = f_o \exp[-\Delta H_o/(RT)]$, where ΔH_o is expected to lie in the range 5.1–11.9 (or more) kcal/mol for complete unstacking and loss of H-bonding at room temperature (Marky & Breslauer, 1982). $\langle\phi^2\rangle_d$ is expected to be a weakly increasing function of T. Thus, $f\langle\phi^2\rangle_d$ is expected to be a strongly increasing function of T. We conclude from the observed temperature invariance of α that high enthalpy perturbed structures do not significantly diminish the overall torsional rigidity of ϕ29 DNA, although we cannot say which of the two requirements cited above is not satisfied.

A critical review of the most pertinent available data concerning spontaneous transient opening of the double helix is given elsewhere (Wilcoxon & Schurr, 1983). Recent formaldehyde kinetics data (Demidov & Lazurkin, 1980) appear to rule out an open base pair intermediate when $T_m - T$ is large; hence, such data can provide only an upper limit for the fraction of open base pairs. An alternative nonopening model with a protonated doorway state is proposed for hydrogen

exchange and provides a good fit to the data with essentially no adjustable parameters. Thermodynamic data from both oligonucleotide studies at room temperature and polynucleotide melting studies indicate a fraction of open base pairs smaller than about 10^{-4}. It is concluded that there is at present no incontrovertible evidence for a fraction of open base pairs greater than about 10^{-4} at room temperature.

If the prevailing value of f is actually as small as 10^{-4}, the open base pairs would not be expected to affect α significantly, unless $\langle\phi^2\rangle_d$ were extremely large. Moreover, if one assumes $\Delta H_o = 9$ kcal/mol, f will increase about 7.3-fold from 25 to 70 °C, so f would still be less than 10^{-3} at 70 °C. These considerations do not prove that f is too small to significantly affect the temperature dependence of α, but they are consistent with that possibility.

On the other hand, if f is as large as 1% at room temperature, as some authors (McGhee & Von Hippel, 1977; Mandal et al., 1979; Manning, 1982) have suggested, then our observations impose significant restrictions upon $\langle\phi^2\rangle_d$. We suppose that the observed temperature dependence of α will remain unaffected by the high-enthalpy open base pairs, provided that $f\langle\phi^2\rangle_d \leq 0.21(1-f)\langle\phi^2\rangle_o$ up to 70 °C. Assuming that $f = 0.01$ and $\Delta H_o = 9$ kcal/mol, we find $\langle\phi^2\rangle_d/\langle\phi^2\rangle_o \leq 2.6$. Thus, the mean-squared angular displacement, which is inversely proportional to the *local* torsion constant, cannot be enhanced more than 2.6-fold at the open base pairs (when $f = 0.01$ and $\Delta H_o = 9$ kcal/mol); otherwise, a significant temperature dependence of α would be observed.

Manning (1983) has recently proposed a model in which bending occurs *exclusively* at sites of high-enthalpy open base pairs. He does not discuss twisting, although that might also be presumed to occur exclusively at the same sites. Manning estimates $f = 0.026$ for these sites, which implies an average rod length of 38 base pairs between joints. Rod lengths of that size for *twisting* of the DNA are ruled out by the functional form of the FPA decay (Thomas et al., 1980a). Moreover, the temperature invariance of α discounts the possibility that twisting occurs predominantly at sites of high-enthalpy open base pairs. Thus, Manning's model evidently requires the DNA to bend in a completely segmental fashion at high-enthalpy kinks, while at the same time it twists in a predominantly smooth or uniform manner.

In fact, the overall bending rigidity is also found to be nearly independent of temperature (Gray & Hearst, 1968; Wilcoxon & Schurr, 1983), which by arguments identical with those given above directly contradicts Manning's model. We note that, in fitting the thermodynamic parameters of his model to the data of Gray and Hearst, Manning has incorrectly assumed that the interkink spacing, and therefore the number of kinks, is a constant independent of temperature. When that error is rectified, one finds that $\Delta H_{\beta d} + \Delta H_o = 288$ cal/mol ~ 0, where $\Delta H_{\beta d}$ is the enthalpy associated with $\langle\beta^2\rangle_d$, the mean-squared bending angle, and ΔH_o is the enthalpy to form an unbent open base pair. Evidently, $\Delta H_{\beta d}$ is constrained to be large and negative to compensate for ΔH_o, which Manning takes to be 5000 ± 1000 cal/mol. The implied rapid decrease of $\langle\beta^2\rangle_d$ with increasing T seems to be a rather physically improbable result. If $\langle\beta^2\rangle_d$ is either a weak or increasing function of T, then any model in which bending occurs predominantly at sites with large and positive ΔH_o is ruled out by the experimental data of Gray & Hearst (1968) or Wilcoxon & Schurr (1983).

Speculation on Premelting Behavior. Although the data in Figure 2 are somewhat noisy, there is the suggestion that α goes through a sudden increase at $T = 70$ °C. This behavior has been observed by us in another ϕ29 DNA solution and may therefore warrant consideration as a real effect. One likely possibility is that, as T_m is approached, the dye vacates the less stable A-T-rich regions and preferentially binds to the more stable G-C-rich regions, which may have slightly higher twisting rigidities. The undiminished value of α observed at 78 °C probably indicates that the dye has vacated the denatured regions in favor of the unmelted double-strand regions at that point.

Another possibility is the following. It has been noted previously that over a narrow region around the melting temperature, DNA actually aggregates (Schmitz & Schurr, 1973; Schurr, 1977; Wilcoxon & Schurr, 1983). A similar observation has been made for collagen (Thomas & Fletcher, 1979), and the idea that this is a general phenomenon exhibited by long multistranded biopolymers cannot be dismissed. Indeed, Shibata & Schurr (1980) have presented a statistical mechanical analysis that explicitly allows aggregation of multistranded biopolymers in the denaturation region. They find that the same secondary bonds responsible for stabilizing the native structure at low temperatures will promote aggregation in the thermal denaturation region for sufficiently long chains. In view of this, we cannot discount the possibility that in the premelt region DNA forms a "cross-linked" aggregate with a concomitant increase in the effective torsion elastic constant.

Conclusion

In this work we find that the torsion elastic constant α for an intact linear DNA is essentially independent of temperature from 10 °C up to the melting temperature $T_m = 76$ °C. This finding parallels the results of our earlier dynamic light scattering measurements on the same DNA in which we found that the bending rigidity was also independent of temperature over a similar temperature range (Wilcoxon & Schurr, 1983). Together, these results argue against any model of DNA flexibility that gives rise to a rigidity that is strongly temperature dependent. The Open-base-pair Kink model of Manning is such a model. We have previously found that neither single-strand breaks nor a large change in the G-C content of DNA substantially alters its flexural and torsional rigidities at neutral pH (Thomas et al., 1980b). All of our data are entirely consistent with the notion that flexibility of duplex DNA results from gradual deformation of its native structure and not primarily from any purely local effect such as kinking or base pair opening. In the light of presently available data, DNA deforms as a smooth elastic filament (Thomas et al., 1980a).

References

Allison, S. A., & Schurr, J. M. (1979) *Chem. Phys. 41*, 35–59.
Allison, S. A., & McCammon, J. A. (1983) *Biopolymers* (in press).
Allison, S. A., Shibata, J. H., Wilcoxon, J., & Schurr, J. M. (1982) *Biopolymers 21*, 729–762.
Barkley, M. D., & Zimm, B. H. (1979) *J. Chem. Phys. 70*, 2991–3007.
Demidov, V. V., & Lazurkin, Yu. S. (1980) *Mol. Biol. (Moscow) 14*, 448–455.
Genest, D., Wahl, P. H., Erard, M., Champagne, M., & Daune, M. (1982) *Biochimie 64*, 419–427.
Gray, H. B., & Hearst, J. E. (1968) *J. Mol. Biol. 35*, 111–129.
Hogan, M., Wang, J., Austin, R. H., Monitto, C., & Herschkowitz, S. (1982) *Proc. Natl. Acad. Sci. U.S.A. 79*, 3518–3522.
Lin, S. C., Thomas, J. C., Allison, S. A., & Schurr, J. M. (1981) *Biopolymers 20*, 209–230.

Magde, D., Zappala, M., Knox, W. H., & Nordlund, T. M. (1983) *J. Phys. Chem. 87*, 3286–3288.
Mandal, C., Kallenbach, N. R., & Englander, S. W. (1979) *J. Mol. Biol. 135*, 391–411.
Manning, G. S. (1983) *Biopolymers 22*, 689–729.
Marky, L. A., & Breslauer, K. J. (1982) *Biopolymers 21*, 2185–2194.
McGhee, J. D., & Von Hippel, P. H. (1977) *Biochemistry 16*, 3276–3293.
Millar, D. P., Robbins, R. J., & Zewail, A. H. (1982) *J. Chem. Phys. 76*, 2080–2094.
Robinson, B. H., Lerman, L. S., Beth, A., Frisch, H. L., Dalton, L. R., & Auer, C. J. (1980) *J. Mol. Biol. 139*, 19–45.
Schmitz, K. S., & Schurr, J. M. (1973) *Biopolymers 12*, 1543–1564.
Schurr, J. M. (1977) *CRC Crit. Rev. Biochem. 4*, 371–431.
Schurr, J. M. (1982) *Chem. Phys. 65*, 417–424.
Schurr, J. M. (1983a) *Chem. Phys.* (in press).
Schurr, J. M. (1983b) *Biopolymers 22*, 2207–2217.
Shibata, J. H., & Schurr, J. M. (1981) *Biopolymers 20*, 525–549.
Thomas, J. C., & Fletcher, G. C. (1979) *Biopolymers 18*, 1333–1352.
Thomas, J. C., & Schurr, J. M. (1979) *Opt. Lett. 4*, 222–223.
Thomas, J. C., Allison, S. A., Appellof, C. J., & Schurr, J. M. (1980a) *Biophys. Chem. 12*, 177–188.
Thomas, J. C., Allison, S. A., Schurr, J. M., & Holder, R. D. (1980b) *Biopolymers 19*, 1451–1474.
Wahl, P. H., Paoletti, J., & LePecq, J.-B. (1970) *Proc. Natl. Acad. Sci. U.S.A. 65*, 417–421.
Wang, J., Hogan, M., & Austin, R. H. (1982) *Proc. Natl. Acad. Sci. U.S.A. 79*, 5896–5900.
Wilcoxon, J., & Schurr, J. M. (1983) *Biopolymers 22*, 2273–2321.
Wilcoxon, J., Shibata, J. H., Thomas, J. C., & Schurr, J. M. (1982) in *Biomedical Applications of Laser Light Scattering* (Sattelle, D. B., Lee, W. I., & Ware, B. R., Eds.) pp 21–35, Elsevier Biomedical Press, Cambridge.

Effects of 3′ Dangling End Stacking on the Stability of GGCC and CCGG Double Helices†

Susan M. Freier, Barbara J. Burger, Dirk Alkema, Thomas Neilson, and Douglas H. Turner*

ABSTRACT: Thermodynamic properties for helix formation of two core molecules, GGCC and CCGG, and pentanucleotides containing either core plus a 3′ dangling nucleotide were measured spectrophotometrically. In 1 M Na^+, the order of stability is GGCC ≈ GGCCp < pGGCC < GGCCC ≈ GGCCCp < GGCCUp < GGCCAp ≈ GGCCGp ≈ GGCCϵAp and CCGG < pCCGG < CCGGCp < CCGGUp < CCGGAp ≈ CCGGGp. In 0.01 M Na^+, the order of stability for the GGCC family does not change except GGCC is more stable than the tetramers with a terminal phosphate. Thermodynamic parameters obtained by using a two-state model demonstrate the stabilizing effect of a 3′ dangling end is enthalpic. The results indicate stacking is an important contributor to nucleic acid stability. Sedimentation equilibrium experiments at 3 °C on GGCCGp in 1 M Na^+ and GGCCAp in 0.01 M Na^+ indicate no aggregation of pentanucleotide helices at strand concentrations as high as 2 mM.

Base stacking is thought to play an important role in the stabilization of nucleic acid helices (Cantor & Schimmel, 1980; Bloomfield et al., 1974; Turner et al., 1981). Stacking in single-strand helices has been extensively studied (Felsenfeld & Miles, 1967; Adler et al., 1967; Brahms et al., 1967a,b; Stannard & Felsenfeld, 1975; Breslauer & Sturtevant, 1977; Filimonov & Privalov, 1978; Suurkuusk et al., 1977; Freier et al., 1981; Dewey & Turner, 1979, 1980; Pörschke, 1973, 1976, 1978). Stacking in double-strand helices can be modeled by addition of a terminal unpaired nucleotide (dangling end) to an oligonucleotide double helix. Addition of a dangling end to an RNA helix stabilizes the helix (Martin et al., 1971; Romaniuk et al., 1978; Neilson et al., 1980; Alkema et al., 1981a,b; Petersheim & Turner, 1983a). In this paper, we report the changes in thermodynamic properties of helix formation associated with attaching various 3′ dangling ends to two core helices, GGCC and CCGG.[1] The results provide insight into the forces stabilizing double helices and should help improve predictions of RNA secondary structure from sequence (Borer et al., 1974).

Materials and Methods

Oligonucleotide Synthesis. GGCC and GGCCC were synthesized from GG (Sigma) by using primer-dependent polynucleotide phosphorylase kindly provided by David Koh. The conditions were similar to those described by Petersheim & Turner (1983a), but no nuclease was added to the reaction mixture. Incubation at 37 °C for 2 days gave the highest yield of tetramer.

CCGG and GGCC were obtained from Collaborative Research. The chromatographic properties and melting curves of the commercial GGCC were identical with those of GGCC

† From the Department of Chemistry, University of Rochester, Rochester, New York 14627 (S.M.F., B.J.B., and D.H.T.), and the Department of Biochemistry, McMaster University, Hamilton, Ontario, L8S 4M1 Canada (D.A. and T.N.). *Received May 24, 1983.* This work was supported by National Institutes of Health Grant GM 22939 and the Medical Research Council of Canada Grant MT-6339. D.H.T. is an Alfred P. Sloan Fellow.

[1] Abbreviations: ATP, adenosine triphosphate; BSA, bovine serum albumin; DEAE, diethylaminoethyl; DTT, dithiothreitol; EDTA, ethylenediaminetetraacetate; HPLC, high-performance liquid chromatography; TEAB, triethylammonium bicarbonate; Tris, tris(hydroxymethyl)-aminomethane; ϵA, 1,N^6-ethenoadenosine. For oligonucleotides, internal phosphates are not denoted; GGC is GpGpC. If a molecule contains a terminal phosphate, it is explicitly indicated.

0006-2960/83/0422-6198$01.50/0